ANZIAM J. 60(2018), 118–136
doi:10.1017/S1446181118000172

EFFECT OF UNIFORM WIND FLOW ON MODULATIONAL INSTABILITY OF TWO CROSSING WAVES OVER FINITE DEPTH WATER

SUMANA KUNDU[✉1], SUMA DEBSARMA[2] and K. P. DAS[2]

(Received 21 August, 2017; accepted 11 January, 2018; first published online 31 August 2018)

Abstract

The effect of uniform wind flow on modulational instability of two crossing waves is studied here. This is an extension of an earlier work to the case of a finite-depth water body. Evolution equations are obtained as a set of three coupled nonlinear equations correct up to third order in wave steepness. Figures presented in this paper display the variation in the growth rate of instability of a pair of obliquely interacting uniform wave trains with respect to the changes in the air-flow velocity, depth of water medium and the angle between the directions of propagation of the two wave packets. We observe that the growth rate of instability increases with the increase in the wind velocity and the depth of water medium. It also increases with the decrease in the angle of interaction of the two wave systems.

2010 *Mathematics subject classification*: primary 76B07; secondary 76B15, 76E17.

Keywords and phrases: crossing seas, evolution equation, gravity waves, instability, wind effect.

1. Introduction

Over the centuries, freak waves remained as marine monsters in the maritime history. Ocean engineer and adventurer Bascom [1] has described some stories of freak waves in his book "Waves and Beaches". In recent years, freak waves, also known as rogue waves, killer waves or giant waves, have become a matter of academic interest. Even today we do not have adequate knowledge of the physics involved in the process of formation of freak waves and the propagation of such waves. Unless these things are clearly understood, prediction of occurrence of these waves is difficult, in spite of applications of sophisticated equipments like radar, drones, satellites, weather information systems, wind's profilers, computers of high configuration and so on.

[1]Salkia Mrigendra Dutta Smriti Balika Vidyapith (High), Salkia, Howrah-711106, India;
e-mail: sumanakundu.mail@gmail.com.
[2]Department of Applied Mathematics, University of Calcutta, 92 A.P.C. Road, Kolkata 700009, India;
e-mail: suma_debsarma@rediffmail.com, kalipada_das@yahoo.com.

Different mathematical models [7, 8, 12, 17, 23, 25] reveal that freak waves can be generated as a result of modulational instability mechanism. Some investigations [11, 13, 16, 18, 20, 24, 31] show how the dynamics of freak waves is influenced by various factors like water current, geometry of the bottom surface, air flowing over the water surface and so on. Chabchoub [4] conducted an experimented with hybrid Peregrine-JONSWAP (Joint North Sea Wave Project) wave field with random phases, and observed formation of an extreme wave.

It is known that waves of different sizes can form even with a fairly steady wind. The factors that determine the size of waves are the wind's speed, the fetch, the duration of wind flow and so on. Miles [21, 22] elaborated a linear theory concerning the initial growth of infinitesimal wind waves. Bliven et al. [2] performed an experiment in a wind-wave tunnel to observe the influence of wind on regular wave growth rate, modulational frequency and sideband growth rate. Dhar and Das [9], Waseda and Tulin [32], Kharif et al. [15], Peirson and Garcia [26] and many others studied influence of wind on water wave propagation. To study evolution of weakly nonlinear gravity waves over finite-depth water in the presence of wind flow, Leblanc [20] added to the Davey–Stewartson [6] equation a linear term corresponding to the Miles mechanism of wave generation. Leblanc found that the modulations of gravity waves grow super-exponentially under the influence of wind. Debsarma et al. [7, 8] also studied asymptotic stability of wind forced modulations in a situation of crossing sea states. They observed super-exponential growth of two obliquely propagating uniform waves as a result of modulational instability. They assumed that the wind input results in a growth rate at an order same as that of the order of nonlinear modulation. In their paper, the effect of wind input is incorporated by adding linear terms proportional to wave steepness to the evolution equations. Chabchoub et al. [5] carried out an experiment in a large wind-wave tank which can generate wind speeds between 1 to 14 ms^{-1}. They found that the evolution of Peregrine solution of nonlinear Schrödinger equation [27] is not much influenced by slow winds blowing in the same direction. They also observed formation of Peregrine breather-like large wave amplitude under the action of strong winds. Brunetti and Kasparian [3] studied the effects of stronger wind-forcing on modulational instability. They considered wind-forced nonlinear Schrödinger equation with a growth rate of the wave energy of the same order as the wave steepness. Such an equation, as observed by Brunetti and Kasparian [3], results in widely extending the spectral range of the modulational instability gain, compared with the wind-forced nonlinear Schrödinger equation with the assumption that the growth rate of the wave energy of the same order as the dissipation. To study statistical properties of wind-generated waves, Toffoli et al. [30] performed an experiment in an annular flume over which a constant and quasi-homogeneous wind blows. In such a tank, waves can propagate circularly in an unlimited fetch condition. They found that the wave field generated in this annular tank in the presence of wind flow deviates largely from the Gaussian statistics. They also observed spontaneous formation of rogue waves just before the wave field reaches a stationary state.

In this paper, we consider a crossing sea states situation at the interface of air and water. We assume that wind flows uniformly over the water body which is of

https://doi.org/10.1017/S1446181118000172 Published online by Cambridge University Press

finite depth. A similar situation was also considered by Senapati et al. [28], but in their paper the water medium was taken to be of infinite depth. Dhar and Das [10] studied evolution of two obliquely interacting water wave packets. They assumed constant atmospheric pressure. Here we assume that the two water wave packets are propagating symmetrically with respect to the direction of wind flow. This assumption makes the model a simple one, but not physically unrealistic. This is because wind-flow direction, in some rare situation, may be half-way between the two directions of water wave propagation. Following a standard multiple scale method, we have derived wind-flow modified evolution equations. Using these evolution equations we have performed stability analysis of a pair of obliquely propagating Stokes wave trains in the presence of wind flowing uniformly over water. The aim of the present study is to see how the presence of wind modifies modulational instability of Stokes wave trains in a situation of crossing sea states. Stability analysis performed here shows that the growth rate of instability increases as the depth of water medium increases. As the wind velocity increases, the growth rate of instability of the two wave trains also increases. We also find that if the angle of interaction of the two wave systems becomes smaller, the growth rate of instability becomes higher.

The paper is organized as follows. In Section 2 we write down the governing equations. In Section 3 we derive the evolution equations, and in Section 4 we present stability analysis of a pair of obliquely propagating uniform wave trains. Finally, in Section 5 we report the results obtained by stability analysis.

2. Basic equations

We consider a finite-depth water body over which wind flows at a uniform speed U parallel to the x-direction. At the interface of air and water, two obliquely propagating narrow-banded water wave packets meet, and produce the wavy interface $z = \zeta(x, y, t)$ at time t. We have chosen z-axis pointing in the vertically upward direction. The simple model that we have considered here is shown in Figure 1. We assume that both air and water medium are inviscid and incompressible, and the motion is irrotational in either medium. Let ϕ_w and ϕ_a be the perturbed velocity potentials in the water medium and atmosphere, respectively. So, the velocity vectors within water and air medium are given, respectively, by $\vec{\nabla}\phi_w$ and $\vec{\nabla}\phi_a + \overrightarrow{U}$, where $\overrightarrow{U} = (U, 0, 0)$. The equations of continuity in water and air medium take the following forms:

$$\nabla^2\phi_w = 0, \quad -h < z < \zeta \tag{2.1}$$

$$\nabla^2\phi_a = 0, \quad \zeta < z < \infty \tag{2.2}$$

where h is the depth of the water body. The kinematic boundary condition at the interface is given by

$$\frac{d}{dt}[z - \zeta(x, y, t)] = 0 \quad \text{on } z = \zeta.$$

Thus, the kinematic boundary conditions at the interface $z = \zeta$ are

$$\frac{\partial\phi_w}{\partial z} - \frac{\partial\zeta}{\partial t} = \frac{\partial\phi_w}{\partial x}\cdot\frac{\partial\zeta}{\partial x} + \frac{\partial\phi_w}{\partial y}\cdot\frac{\partial\zeta}{\partial y} \quad \text{on } z = \zeta, \tag{2.3}$$

https://doi.org/10.1017/S1446181118000172 Published online by Cambridge University Press

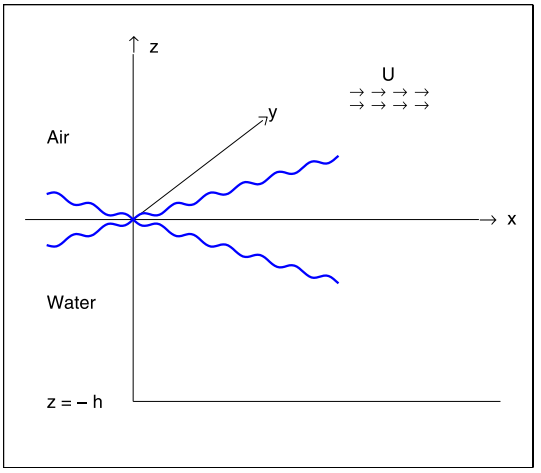

FIGURE 1. Schematic description of the model of crossing seas in the presence of wind blowing uniformly over water.

$$\frac{\partial \phi_a}{\partial z} - \frac{\partial \zeta}{\partial t} - U\frac{\partial \zeta}{\partial x} = \frac{\partial \phi_a}{\partial x}\cdot\frac{\partial \zeta}{\partial x} + \frac{\partial \phi_a}{\partial y}\cdot\frac{\partial \zeta}{\partial y} \quad \text{on } z = \zeta\cdot \tag{2.4}$$

The equations of motion in the water and air medium are, respectively,

$$\frac{d}{dt}[\vec{\nabla}\phi_w] = \overrightarrow{g} - \frac{1}{\rho_w}\vec{\nabla}p_w,$$

$$\frac{d}{dt}[\vec{\nabla}\phi_a + \overrightarrow{U}] = \overrightarrow{g} - \frac{1}{\rho_a}\vec{\nabla}p_a,$$

where ρ_a, ρ_w are the densities of air and water medium, respectively; p_a, p_w are the pressure of air and water medium, respectively, and $\overrightarrow{g}$ is the acceleration due to the earth's gravity. The condition of continuity of pressure at the air–water interface gives $p_w = p_a$ on $z = \zeta$. This gives the dynamic boundary condition

$$\rho_w\frac{\partial \phi_w}{\partial t} - \rho_a\frac{\partial \phi_a}{\partial t} + g(\rho_w - \rho_a)\zeta - \rho_a U\frac{\partial \phi_a}{\partial x} = -\frac{1}{2}\rho_w(\vec{\nabla}\phi_w)^2 + \frac{1}{2}\rho_a(\vec{\nabla}\phi_a)^2 \quad \text{on } z = \zeta. \tag{2.5}$$

The bottom boundary condition is

$$\frac{\partial \phi_w}{\partial z} = 0 \quad \text{on } z = -h. \tag{2.6}$$

In the atmospheric medium,

$$\phi_a \to 0 \quad \text{as } z \to \infty. \tag{2.7}$$

To obtain linear dispersion relation for the system of equations (2.1)–(2.7), we consider the motion of an infinitesimal progressive wave with wave number (k, l) and frequency ω at the air–water interface in the following form:

$$\zeta = \alpha\sin(kx + ly - \omega t),$$

https://doi.org/10.1017/S1446181118000172 Published online by Cambridge University Press

$$\phi_a = \alpha_a(z)\cos(kx + ly - \omega t),$$
$$\phi_w = \alpha_w(z)\cos(kx + ly - \omega t).$$

Substituting these in the linearized version of equations (2.1)–(2.7) and then eliminating α, α_a, α_w, we obtain the following linear dispersion relation:

$$D(\omega, k, l) \equiv \omega^2 \coth(h\sqrt{k^2 + l^2}) + r(\omega - Uk)^2 - g(1 - r)\sqrt{k^2 + l^2} = 0, \tag{2.8}$$

where $r = \rho_a/\rho_w$ is the density ratio. Since equation (2.8) is quadratic in ω, there are two possible modes of wave propagation for the following two values of ω:

$$\omega_\pm = \frac{rUk\tanh(k_c h) \pm \sqrt{[g(1 - r)k_c\{1 + r\tanh(k_c h)\} - rk^2U^2]\tanh(k_c h)}}{1 + r\tanh(k_c h)}, \tag{2.9}$$

where $k_c = \sqrt{k^2 + l^2}$. We may designate waves to be of positive mode or negative mode according as they propagate with frequency $\omega = \omega_+$ or $\omega = \omega_-$. Expression (2.9) for $\omega_\pm$ also shows that a wave with wave number (k, l) becomes linearly unstable, if the wind-flow velocity exceeds the critical velocity U_c, which is given by

$$U_c = \left[\frac{gk_c(1 - r)\{1 + r\tanh(k_c h)\}}{rk^2}\right]^{1/2}. \tag{2.10}$$

When the wave propagates making an angle θ with the direction of air flow $k = k_c\cos\theta$, $l = k_c\sin\theta$ and equation (2.10) becomes

$$U_c\cos\theta = \left[\frac{g(1 - r)\{1 + r\tanh(k_c h)\}}{rk_c}\right]^{1/2}.$$

In Figure 2 we have shown the variation of critical velocity U_c with respect to characteristic wave number k_c for a given depth $h = 500$ m. Considering limit $h \to \infty$ in (2.10), we can find the critical velocity U_c for infinite-depth water, which is

$$U_c = \left[\frac{gk_c(1 - r^2)}{rk^2}\right]^{1/2}.$$

In the present model, we assume that the magnitude of the wind-flow velocity is much less than this critical velocity U_c, which assures us that the waves do not undergo linear instability mechanism. Note that a wind-wave can be of various forms depending on the nature (magnitude or direction) of the wind flow. A detailed discussion on the generation of waves by wind and the interaction of ocean waves with wind was given by Janssen [14].

3. Derivation of evolution equations

We have considered weakly nonlinear interaction of two narrow-banded water wave packets having central wave numbers (k, l) and $(k, -l)$. Above the water surface wind flows with a uniform velocity U in a direction parallel to the x-axis. Thus, in our ocean model, the two wave packets are propagating symmetrically with respect to the

https://doi.org/10.1017/S1446181118000172 Published online by Cambridge University Press

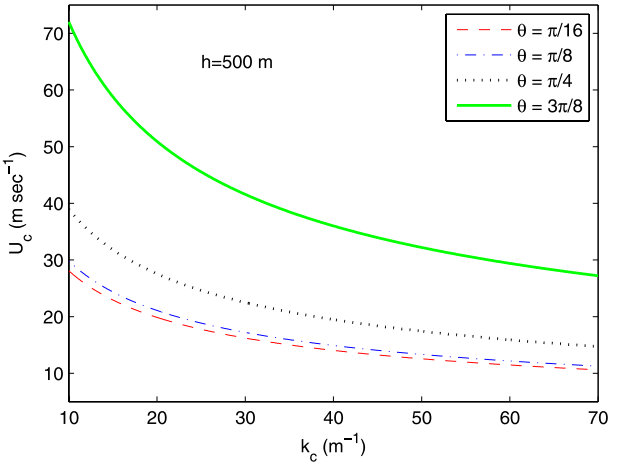

FIGURE 2. Plot of critical velocity U_c against carrier wave number k_c for different values of θ and for $r = 0.00129$, $h = 500$ m.

direction of wind flow. In order to derive the wind-flow modified evolution equations in a situation of crossing sea states, here we have followed standard multiple scale method as in Dhar and Das [10]. We assume a solution of equations (2.1)–(2.7) in the form

$$\phi_w = \phi_{00} + \sum_{(m,n)\neq(0,0)} [\phi_{mn} \exp\{i(m\psi_1 + n\psi_2)\} + \text{c.c.}], \tag{3.1}$$

$$\phi_a = \phi'_{00} + \sum_{(m,n)\neq(0,0)} [\phi'_{mn} \exp\{i(m\psi_1 + n\psi_2)\} + \text{c.c.}], \tag{3.2}$$

$$\zeta = \zeta_{00} + \sum_{(m,n)\neq(0,0)} [\zeta_{mn} \exp\{i(m\psi_1 + n\psi_2)\} + \text{c.c.}], \tag{3.3}$$

where $\psi_1 = kx + ly - \omega t$ and $\psi_2 = kx - ly - \omega t$ are the phase functions of the first and second wave packets, respectively. Note that (ω, k, l) and $(\omega, k, -l)$ both satisfy the linear dispersion relation (2.8). Here c.c. is the abbreviation for complex conjugate, and ϕ_{mn}, ϕ'_{mn} are functions of x_1, y_1, z and t_1 while ζ_{mn} are functions of x_1, y_1 and t_1. Here x_1, y_1, t_1 are slow space and time variables defined by

$$x_1 = \epsilon x, \quad y_1 = \epsilon y, \quad t_1 = \epsilon t,$$

where the parameter ϵ indicates the order of smallness of wave steepness.

Substituting (3.1) and (3.2) in equations (2.1) and (2.2), respectively, and then equating coefficients of $\exp[i(m\psi_1 + n\psi_2)]$ on both sides of these two equations, we get the following equations for ϕ_{mn} and ϕ'_{mn} with $(m, n) = (0, 0), (1, 0), (0, 1), (1, 1), (1, -1), (2, 0)$ and $(0, 2)$:

$$\left[\frac{d^2}{dz^2} - \Delta^2_{mn}\right](\phi_{mn}, \phi'_{mn}) = (0, 0), \tag{3.4}$$

https://doi.org/10.1017/S1446181118000172 Published online by Cambridge University Press

where

$$\Delta_{mn}^2 \equiv K_{mn}^2 + L_{mn}^2, \quad K_{mn} \equiv \left\{(m+n)k - i\epsilon\frac{\partial}{\partial x_1}\right\}, \quad L_{mn} \equiv \left\{(m-n)l - i\epsilon\frac{\partial}{\partial y_1}\right\}.$$

Condition (2.6) requires

$$\frac{\partial \phi_{mn}}{\partial z} = 0 \quad \text{on } z = -h, \tag{3.5}$$

while condition (2.7) demands

$$\phi'_{mn} \to 0 \quad \text{as } z \to \infty. \tag{3.6}$$

The general solution of (3.4), which satisfies end conditions (3.5) and (3.6) are

$$\phi_{mn} = \cosh[(z+h)\Delta_{mn}]A_{mn},$$

$$\phi'_{mn} = \exp[-z\Delta_{mn}]A'_{mn}, \quad (m,n) \neq (0,0),$$

where A_{mn} and A'_{mn} are functions of x_1, y_1 and t_1.

For convenience, we take Fourier transforms of zeroth harmonic equations in (3.4) (that is, for $(m,n) = (0,0)$), with respect to x_1 and y_1, defined by

$$\bar{f}(\kappa_x, \kappa_y) = \frac{1}{2\pi}\int\int_{-\infty}^{\infty} f(x_1, y_1)\exp[-i\kappa_x x_1 - i\kappa_y y_1]\,dx_1\,dy_1,$$

where κ_x and κ_y are Fourier transform parameters. Performing the Fourier transform we obtain

$$\left[\frac{d^2}{dz^2} + \epsilon^2\kappa^2\right](\bar{\phi}_{00}, \bar{\phi}'_{00}) = (0,0), \tag{3.7}$$

where $\kappa^2 = \kappa_x^2 + \kappa_y^2$.

Recalling the end conditions (3.5) and (3.6), we take solution of equations (3.7) as

$$\bar{\phi}_{00} = \cosh[\epsilon\kappa(h+z)]\bar{A}_{00}, \tag{3.8}$$

$$\bar{\phi}'_{00} = \exp[-\epsilon\kappa z]\bar{A}'_{00}, \tag{3.9}$$

where $\bar{A}_{00}$ and $\bar{A}'_{00}$ are functions of κ_x, κ_y and t_1. We now expand (2.3), (2.4) and (2.5) in Taylor's series about $z = 0$ and then in the resulting equations we substitute (3.1)–(3.3) and also use solutions (3.8)–(3.9). Finally, equating coefficients of $\exp[i(m\psi_1 + n\psi_2)]$ on both sides, we get the following system of equations:

$$\Delta_{mn}\sinh(h\Delta_{mn})A_{mn} + iW_{mn}\zeta_{mn} = a_{mn}, \tag{3.10}$$

$$-\Delta_{mn}A'_{mn} + iW_{mn}\zeta_{mn} - iUK_{mn}\zeta_{mn} = a'_{mn}, \tag{3.11}$$

$$-iW_{mn}\cosh(h\Delta_{mn})A_{mn} + irW_{mn}A'_{mn} + g(1-r)\zeta_{mn} - irUK_{mn}A'_{mn} = b_{mn} \tag{3.12}$$

on $z = 0$ with

$$W_{mn} \equiv (m+n)\omega + i\epsilon\frac{\partial}{\partial t_1},$$

and a_{mn}, a'_{mn}, b_{mn} as contributions from nonlinear terms. Fourier transforms of zeroth harmonic equations in (3.10)–(3.12) yield the following three equations:

https://doi.org/10.1017/S1446181118000172 Published online by Cambridge University Press

$$\epsilon k \sinh(\epsilon kh)\bar{A}_{00} - \epsilon\frac{\partial\bar{\zeta}_{00}}{\partial t_1} = \bar{a}_{00}, \tag{3.13}$$

$$-\epsilon k\bar{A}'_{00} - \epsilon\frac{\partial\bar{\zeta}_{00}}{\partial t_1} - i\epsilon U k_x\bar{\zeta}_{00} = \bar{a}'_{00}, \tag{3.14}$$

$$\epsilon\cosh(\epsilon kh)\frac{\partial\bar{A}_{00}}{\partial t_1} - \epsilon r\frac{\partial\bar{A}'_{00}}{\partial t_1} + g(1-r)\bar{\zeta}_{00} - i\epsilon U r k_x\bar{A}'_{00} = \bar{b}_{00} \tag{3.15}$$

on $z = 0$. Eliminating $\bar{A}_{00}$, $\bar{A}'_{00}$ from equations (3.10)–(3.12) for $(m, n) = (1, 0)$ and $(0, 1)$ we obtain the following equations:

$$\begin{aligned}&[\{\coth(h\Delta_{mn}) + r\}W_{mn}^2 - 2\rho U K_{mn}W_{mn} + rU^2K_{mn}^2 - g(1-\rho)\Delta_{mn}]\zeta_{mn}\\ &\quad = -iW_{mn}\coth(h\Delta_{mn})a_{mn} - ir(W_{mn} - UK_{mn})a'_{mn} - \Delta_{mn}b_{mn}\end{aligned} \tag{3.16}$$

for $(m, n) = (1, 0), (0, 1)$. We make use of the two equations in equation (3.16) to determine the evolution equations of the two water wave packets considered in this section. For that we need solutions for $\bar{A}_{mn}$, $\bar{A}'_{mn}$ and ζ_{mn} for $(m, n) = (1, 0), (0, 1), (2, 0), (0, 2), (1, 1), (1, -1), (0, 0)$. We take perturbation expansion of these quantities in the form

$$G_{mn} = \Sigma\epsilon^p G_{mn}^{(p)},$$

where G_{mn} stands for $\bar{A}_{mn}$, $\bar{A}'_{mn}$ and ζ_{mn}, and the superscript p starts from $p = 1$ for $(m, n) = (1, 0), (0, 1)$ and it starts from $p = 2$ for the other variables. Solutions for $\bar{A}_{mn}$, $\bar{A}'_{mn}$ and ζ_{mn} are given in Appendix A. We now solve equations (3.13)–(3.15) for the case $(m, n) = (0, 0)$. Having determined a_{00}, a'_{00} and b_{00} we note that a_{00}, a'_{00} are of $O(\epsilon^3)$ while b_{00} is of $O(\epsilon^2)$. Thus, from equation (3.15) we conclude that $\bar{\zeta}_{00}$ is of $O(\epsilon^2)$. Also, from equations (3.13) and (3.14) we conclude that $\bar{A}_{00}$ is of $O(\epsilon)$ and $\bar{A}'_{00}$ is of $O(\epsilon^2)$. Solving equations (3.13)–(3.15) we get $\bar{A}_{00}$, $\bar{A}'_{00}$ and $\bar{\zeta}_{00}$, which are given in Appendix A. Finally, we substitute all the solutions obtained above on the right-hand side of two equations in (3.16) and simplify both sides correct up to $O(\epsilon^3)$. Thus, we obtain the following equations which govern the evolution of the two wave packets having carrier wave numbers (k, l) and $(k, -l)$, when they interact in a situation in which air flows with uniform velocity parallel to x-direction. These equations are then made dimensionless by using the following changes of variables:

$$\begin{aligned}&x'_1 = k_c x_1, \quad y'_1 = k_c y_1, \quad t'_1 = t_1\sqrt{gk_c\sigma}, \quad \sigma = \tanh(k_c h), \quad k_c = \sqrt{k^2 + l^2},\\ &\zeta'_{10} = k_c\zeta_{10}, \quad \zeta'_{01} = k_c\zeta_{01}, \quad U' = U/\sqrt{g\sigma/k_c}, \quad E = A_{00}^{(1)}/(\sqrt{gk_c\sigma}/k_c^2),\\ &h' = k_c h, \quad k' = k/k_c, \quad l' = l/k_c, \quad \omega' = \omega/\sqrt{gk_c\sigma}.\end{aligned}$$

In dimensionless form the evolution equations, correct up to third order in wave steepness, are the following in which we have dropped the ($'$) notation:

$$\begin{aligned}&i\frac{\partial\zeta_{10}}{\partial t_1} + i\beta_1\frac{\partial\zeta_{10}}{\partial x_1} + i\beta_2\frac{\partial\zeta_{10}}{\partial y_1} + \beta_3\frac{\partial^2\zeta_{10}}{\partial x_1^2} + \beta_4\frac{\partial^2\zeta_{10}}{\partial y_1^2} + \beta_5\frac{\partial^2\zeta_{10}}{\partial x_1\partial y_1}\\ &\quad = \lambda_1\zeta_{10}^2\zeta_{10}^* + \lambda_2\zeta_{10}\zeta_{01}\zeta_{01}^* + \lambda_3\zeta_{10}L_+E,\end{aligned} \tag{3.17}$$

https://doi.org/10.1017/S1446181118000172 Published online by Cambridge University Press

$$i\frac{\partial\zeta_{01}}{\partial t_1} + i\beta_1\frac{\partial\zeta_{01}}{\partial x_1} - i\beta_2\frac{\partial\zeta_{01}}{\partial y_1} + \beta_3\frac{\partial^2\zeta_{01}}{\partial x_1^2} + \beta_4\frac{\partial^2\zeta_{01}}{\partial y_1^2} - \beta_5\frac{\partial^2\zeta_{01}}{\partial x_1\partial y_1}$$
$$= \lambda_1\zeta_{01}^2\zeta_{01}^* + \lambda_2\zeta_{01}\zeta_{10}\zeta_{10}^* + \lambda_3\zeta_{01}L_-E, \tag{3.18}$$

where E satisfies the equation

$$\left[\sigma^2\frac{\partial^2}{\partial t_1^2} - (1-r)h\sigma\left(\frac{\partial^2}{\partial x_1^2} + \frac{\partial^2}{\partial y_1^2}\right)\right]E = L_+(\zeta_{10}\zeta_{10}^*) + L_-(\zeta_{01}\zeta_{01}^*). \tag{3.19}$$

The operators $L_\pm$ appearing in equations (3.17)–(3.19) are

$$L_\pm \equiv 2(1-r)\omega\left(k\frac{\partial}{\partial x_1} \pm l\frac{\partial}{\partial y_1}\right) - (1-\sigma^2)\omega^2\frac{\partial}{\partial t_1}.$$

The coefficients β_i, λ_i are given in Appendix B. In the absence of wind flow we recover the evolution equations of Kundu et al. [18]. Also, in the limit $h \to \infty$, these coefficients are in agreement with the corresponding coefficients of Senapati et al. [28].

We now introduce a reference frame that moves horizontally along positive the x-direction with a velocity equal to the group-velocity component of either wave packet in that direction. The new space and time variables are

$$\xi = x_1 - kc_g t_1, \quad \eta = y_1, \quad \tau = \epsilon t_1,$$

where c_g is the dimensionless group velocity given by $kc_g = \partial\omega/\partial k = \beta_1$. In this moving reference frame, equations (3.17)–(3.19) become, respectively,

$$i\frac{\partial\zeta_{10}}{\partial\tau} + i\beta_2\frac{\partial\zeta_{10}}{\partial\eta} + \beta_3\frac{\partial^2\zeta_{10}}{\partial\xi^2} + \beta_4\frac{\partial^2\zeta_{10}}{\partial\eta^2} + \beta_5\frac{\partial^2\zeta_{10}}{\partial\xi\partial\eta}$$
$$= \lambda_1\zeta_{10}^2\zeta_{10}^* + \lambda_2\zeta_{10}\zeta_{01}\zeta_{01}^* + \lambda_3\zeta_{10}L_+E, \tag{3.20}$$

$$i\frac{\partial\zeta_{01}}{\partial\tau} - i\beta_2\frac{\partial\zeta_{01}}{\partial\eta} + \beta_3\frac{\partial^2\zeta_{01}}{\partial\xi^2} + \beta_4\frac{\partial^2\zeta_{01}}{\partial\eta^2} - \beta_5\frac{\partial^2\zeta_{01}}{\partial\xi\partial\eta}$$
$$= \lambda_1\zeta_{01}^2\zeta_{01}^* + \lambda_2\zeta_{01}\zeta_{10}\zeta_{10}^* + \lambda_3\zeta_{01}L_-E, \tag{3.21}$$

$$\mu_1\frac{\partial^2E}{\partial\xi^2} + \mu_2\frac{\partial^2E}{\partial\eta^2} = L_+(\zeta_{10}\zeta_{10}^*) + L_-(\zeta_{01}\zeta_{01}^*). \tag{3.22}$$

The coefficients μ_1 and μ_2 are given in Appendix B. These two coefficients match the corresponding coefficients of equation (32) of Kundu et al. [18]. The operators $L_\pm$ appearing in equations (3.20)–(3.22) now have the form

$$L_\pm \equiv \{2k\omega(1-r) + \beta_1(1-\sigma^2)\omega^2\}\frac{\partial}{\partial\xi} \pm 2l\omega(1-r)\frac{\partial}{\partial\eta}.$$

In the absence of air flow and second wave packet, the system of equations (3.20)–(3.22) reduce to Davey–Stewartson [6] equations. Again, if we consider limit $h \to \infty$ in the absence of airflow, then the coefficients β_i, λ_i become in agreement with the

https://doi.org/10.1017/S1446181118000172 Published online by Cambridge University Press

corresponding coefficients of the evolution equations derived by Onorato et al. [23] and Shukla et al. [29].

For very small h, the coefficients $\beta_1, \beta_2, \beta_3, \beta_4, \beta_5$ are of order $O(h^{-1/2})$, $O(h^{-1/2})$, $O(h^{-3/2})$, $O(h^{-3/2})$ and $O(h^{-3/2})$, respectively; while the coefficients λ_1, λ_2, λ_3, μ_1 and μ_2 are of order $O(h^{-3/2})$, $O(h^{-3/2})$, $O(h^{-1/2})$, $O(h^2)$, $O(h^2)$, respectively. So, the evolution equations (3.20)–(3.22) do not remain valid for shallow water body.

4. Stability analysis

Spatially uniform solution of the system of equations (3.20)–(3.22) is given by

$$\zeta_{10} = A_0 e^{-i\tau\Delta\omega_1}, \quad \zeta_{01} = B_0 e^{-i\tau\Delta\omega_2}, \quad E = E_0, \tag{4.1}$$

where A_0, B_0 and E_0 are three real constants. The amplitude dependent frequency shifts of the two wavetrains are given by

$$\Delta\omega_1 = \lambda_1 A_0^2 + \lambda_2 B_0^2, \quad \Delta\omega_2 = \lambda_1 B_0^2 + \lambda_2 A_0^2.$$

To investigate stability of the above uniform solution (4.1), we consider the following infinitesimal perturbation:

$$\zeta_{10} = A_0 e^{-i\tau\Delta\omega_1}(1 + A'), \quad \zeta_{01} = B_0 e^{-i\tau\Delta\omega_2}(1 + B'), \quad E = E_0(1 + E'). \tag{4.2}$$

We now substitute the perturbed solution (4.2) in equations (3.20)–(3.22) and linearize with respect to the perturbed quantities. Assuming

$$A' = A'_r + iA'_i, \quad B' = B'_r + iB'_i, \quad E' = E'_r + iE'_i,$$

with $A'_r, A'_i, B'_r, B'_i, E'_r, E'_i$ being real, we separate real and imaginary parts. Thereby, we get a system of six equations in these perturbed variables. Then we take the Fourier transform of these equations with respect to ξ, with η defined by

$$\bar{f}(K, L) = \frac{1}{2\pi} \int\int_{-\infty}^{\infty} f(\xi, \eta) e^{-i(K\xi + L\eta)}\, d\xi\, d\eta,$$

where f stands for $A'_r, A'_i, B'_r, B'_i, E'_r$, and E'_i. Finally, assuming time dependence of $\bar{A}'_r, \bar{A}'_i, \bar{B}'_r, \bar{B}'_i, \bar{E}'_r$ and $\bar{E}'_i$ to be of the form $\exp(-i\Omega\tau)$ we obtain the following linear system of six equations:

$$(\beta_3 K^2 + \beta_4 L^2 + \beta_5 KL + 2\lambda_1 A_0^2)\bar{A}'_r - i(\Omega - \beta_2 L)\bar{A}'_i + 2\lambda_2 B_0^2 \bar{B}'_r + iE_0\lambda_3 Q_+ \bar{E}'_r = 0, \tag{4.3}$$

$$i(\Omega - \beta_2 L)\bar{A}'_r + (\beta_3 K^2 + \beta_4 L^2 + \beta_5 KL + 2\lambda_1 A_0^2)\bar{A}'_i + iE_0\lambda_3 Q_+ \bar{E}'_i = 0, \tag{4.4}$$

$$2\lambda_2 A_0^2 \bar{A}'_r + (\beta_3 K^2 + \beta_4 L^2 - \beta_5 KL + 2\lambda_1 B_0^2)\bar{B}'_r - i(\Omega + \beta_2 L)\bar{B}'_i + iE_0\lambda_3 Q_- \bar{E}'_r = 0, \tag{4.5}$$

$$i(\Omega + \beta_2 L)\bar{B}'_r + (\beta_3 K^2 + \beta_4 L^2 - \beta_5 KL)\bar{B}'_i + iE_0\lambda_3 Q_- \bar{E}'_i = 0, \tag{4.6}$$

$$2iA_0^2 Q_+ \bar{A}'_r + 2iB_0^2 Q_- \bar{B}'_r + (\mu_1 K^2 + \mu_2 L^2)E_0 \bar{E}'_r = 0, \tag{4.7}$$

$$(\mu_1 K^2 + \mu_2 L^2)E_0 \bar{E}'_i = 0. \tag{4.8}$$

https://doi.org/10.1017/S1446181118000172 Published online by Cambridge University Press

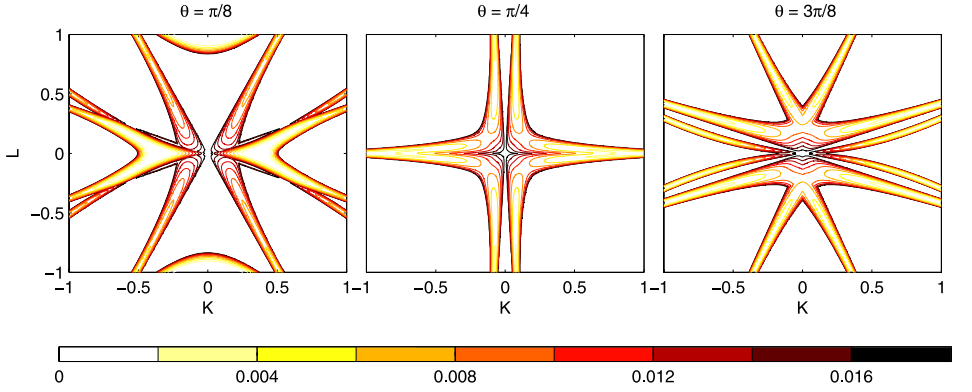

FIGURE 3. Contour plot of G_r in K–L plane $r = 0.00129$, $U = 10$, $A_0 = 0.1$, $B_0 = 0.1$, $h = 2$.

The factor $(\mu_1 K^2 + \mu_2 L^2)$ vanishes only if $(K, L) = (0, 0)$ or if $h = 0$. Hence, from equation (4.8) it follows that $\bar{E}_i' = 0$. Again, using (4.7) we can eliminate $\bar{E}_r'$ from the equation (4.3)–(4.6). As a result, the system of six equations (4.3)–(4.8) reduces to a system of four equations in four unknowns $\bar{A}_r'$, $\bar{A}_i'$, $\bar{B}_r'$, $\bar{B}_i'$. This system possesses a nontrivial solution only if Ω satisfies the following biquadratic equation

$$\begin{aligned}&[(\Omega - \beta_2 L)^2 - P_+\{P_+ + 2(\lambda_1 + \lambda_3 Q_+^2 R)A_0^2\}]\\ &\qquad \cdot [(\Omega + \beta_2 L)^2 - P_-\{P_- + 2(\lambda_1 + \lambda_3 Q_-^2 R)B_0.^2\}]\\ &\quad = 4P_+P_-(\lambda_2 + \lambda_3 Q_+ Q_- R)^2 A_0^2 B_0^2. \end{aligned} \tag{4.9}$$

Equation (4.9) is the nonlinear dispersion relation in which $P_\pm$, $Q_\pm$, R are

$$\begin{aligned}P_\pm &= \beta_3 K^2 + \beta_4 L^2 \pm \beta_5 KL,\\ Q_\pm &= [2k\omega(1 - r) + \beta_1(1 - \sigma^2)\omega^2]K \pm 2l\omega(1 - r)L,\\ R &= [\mu_1 K^2 + \mu_2 L^2]^{-1}.\end{aligned}$$

Solving equation (4.9) numerically we have plotted growth rate of instability $G_r = \mathrm{Im}(\Omega)$ of the uniform wave solution (4.1) in the perturbed wave number plane.

In Figures 3–6 we have shown contour plots of growth rate of instability for $\theta = \pi/8$, $\pi/4$, $3\pi/8$. Following Leblanc [19], we have chosen $r = 0.00129$ as the density ratio between air and water. In Figures 3–5 the amplitudes of the two wave trains are taken to be equal $A_0 = B_0 = 0.1$, while in Figure 6, $A_0 = 0.12$, $B_0 = 0.07$. Figures 3, 4, 6 are drawn for positive mode of wave propagation taking $U = 10$, while Figure 5 is for the case of negative mode of wave propagation taking $U = -10$. If we compare Figure 4 with Figure 5, we observe that the region of instability expands as the depth of the water medium increases within the scope of validity of the evolution equations (3.20)–(3.22). Comparing Figure 5 with Figure 3, we observe that there is not much difference in the regions of instability for the positive and negative modes of wave propagation.

https://doi.org/10.1017/S1446181118000172 Published online by Cambridge University Press

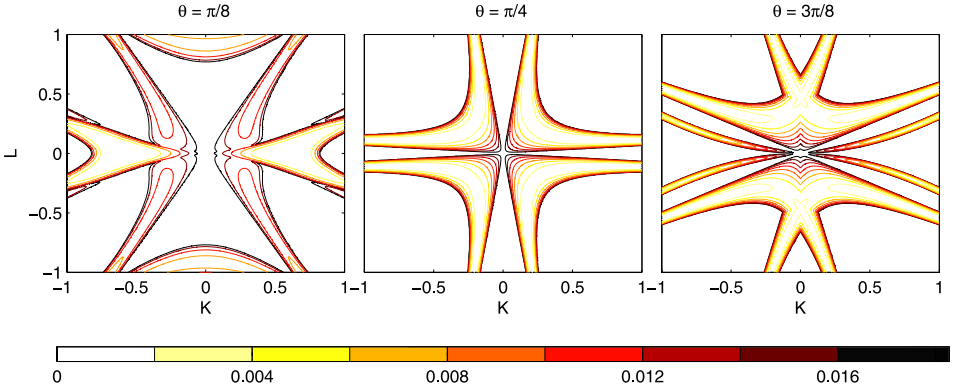

FIGURE 4. Contour plot of G_r in K–L plane $r = 0.00129$, $U = 10$, $A_0 = 0.1$, $B_0 = 0.1$, $h = 5$.

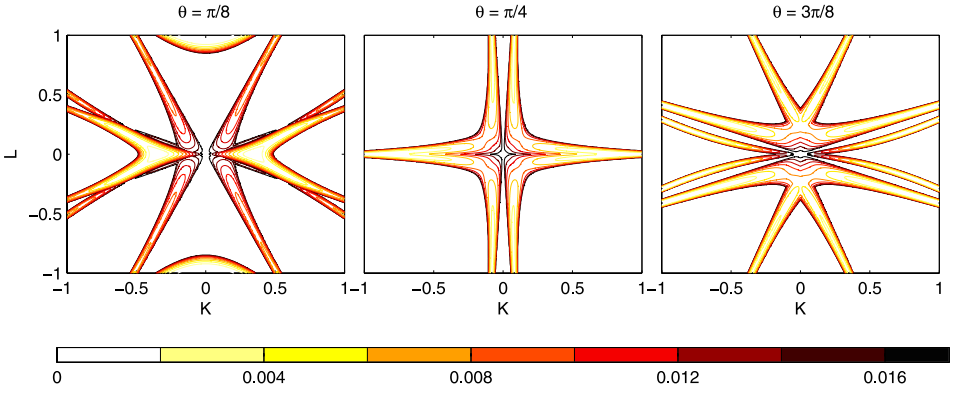

FIGURE 5. Contour plot of G_r in K–L plane $r = 0.00129$, $U = -10$, $A_0 = 0.1$, $B_0 = 0.1$, $h = 2$.

For unidirectional perturbations along x-direction, equation (4.9) can be solved for Ω as follows:

$$\Omega^2 = \beta_3 K^2[\beta_3 K^2 + (\lambda_1 + \lambda_3 S)(A_0^2 + B_0^2) \pm \sqrt{\{(\lambda_1 + \lambda_3 S)(A_0^2 - B_0^2)\}^2 + 4(\lambda_2 + \lambda_3 S)^2 A_0^2 B_0^2}],$$

where

$$S = [2k\omega(1 - r) + \beta_1(1 - \sigma^2)\omega^2]^2/\mu_1.$$

The uniform wave solution (4.1) becomes unstable under perturbation along x-direction when

$$\beta_3[(\lambda_1 + \lambda_3 S)(A_0^2 + B_0^2) \pm \sqrt{\{(\lambda_1 + \lambda_3 S)(A_0^2 - B_0^2)\}^2 + 4(\lambda_2 + \lambda_3 S)^2 A_0^2 B_0^2}] < 0.$$

Figure 7 shows stable and unstable regions in h–θ plane for unidirectional perturbations. Comparing the right-hand figure ($U = 10$) with left-hand figure ($U = 5$)

https://doi.org/10.1017/S1446181118000172 Published online by Cambridge University Press

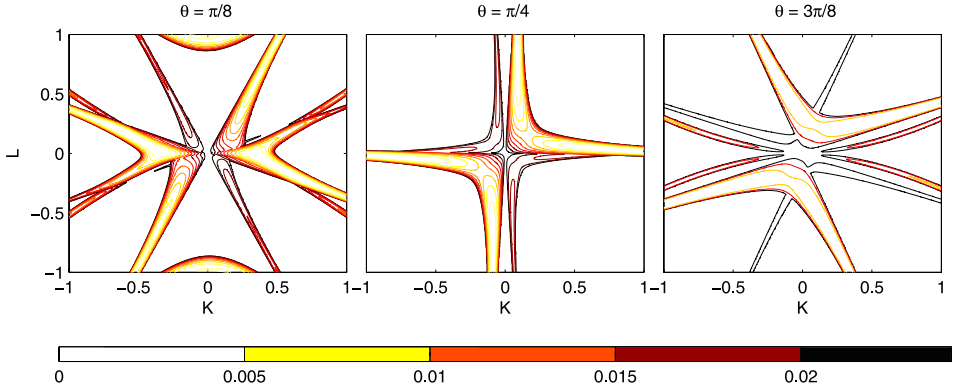

FIGURE 6. Contour plot of G_r in K–L plane $r = 0.00129$, $U = 10$, $A_0 = 0.12$, $B_0 = 0.07$, $h = 2$.

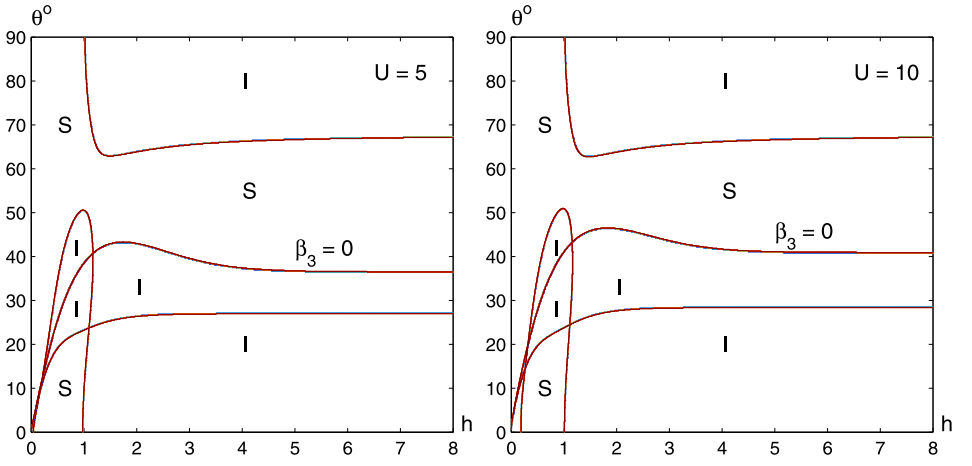

FIGURE 7. Stability and instability regions in h–θ plane for unidirectional perturbations: S denotes stability and I denotes instability; $U = 5$ (left), $U = 10$ (right).

in Figure 7 we find that the curve $\beta_3 = 0$ lies at a little bit upper position in the right-hand figure, which implies that the region of instability increases with the increase in wind-flow velocity. In Figures 8–11 we have shown the variation in growth rate of instability $G_r = \mathrm{Im}(\Omega)$ against perturbation wave number K for different values of U, θ and h. In all the Figures 8–11 it is observed that G_r initially increases with the increase in perturbation wave number K, but then it starts diminishing. In Figure 8 we have plotted growth rate of instability $G_r = \mathrm{Im}(\Omega)$ against perturbation wave number K for different values of wave steepness B_0 of the second wave train. We see that G_r increases with the increase in B_0. In Figure 9 we have shown the variation in G_r with respect to the change in angle θ. It is seen that G_r decreases with the increase in the half-angle θ between the directions of propagation of the two wave trains.

https://doi.org/10.1017/S1446181118000172 Published online by Cambridge University Press

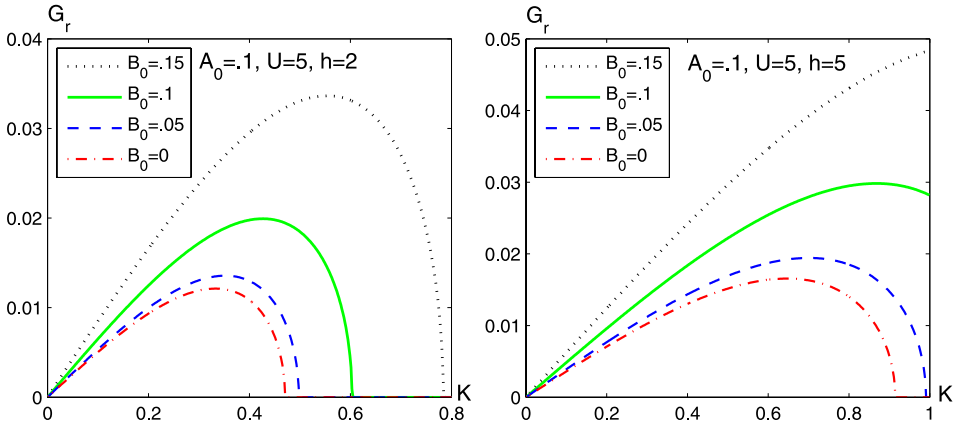

FIGURE 8. G_r vs K, $r = 0.00129$, $\theta = \pi/6$, $U = 5$, $A_0 = 0.1$, $B_0 = 0, 0.05, 0.1, 0.15$, $h = 2$ (left), $h = 5$ (right).

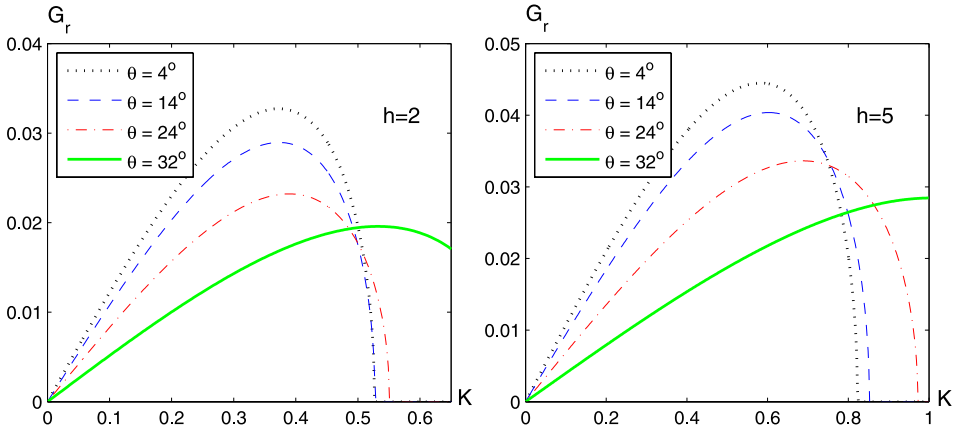

FIGURE 9. G_r vs K, $r = 0.00129$, $A_0 = 0.12$, $B_0 = 0.07$, $U = 5$, $\theta = 4°, 14°, 24°, 32°$, $h = 2$ (left), $h = 5$ (right).

Comparing the right-hand figure with the corresponding left-hand figure in Figures 8–11, we observe that the maximum growth rate of instability is higher for $h = 5$ compared with that for $h = 2$. Figure 10 shows how G_r changes as the wind-flow velocity changes. Note that G_r increases with the increase in air-flow velocity, both for the positive and negative modes of wave propagation. In Figure 11 we observe the variation in G_r with respect to the change in water depth $1.2 \leq h \leq 2.2$. We find that G_r increases with the increase in water depth. In Figures 8–11 we observe that as the depth of water medium increases, the growth rate of instability becomes maximum for larger values of perturbation wavenumber. Since we have considered here linear stability of the uniform solution given by (4.1), we should keep in mind that all the results of stability analysis remain valid only for sufficiently small perturbation wave numbers.

https://doi.org/10.1017/S1446181118000172 Published online by Cambridge University Press

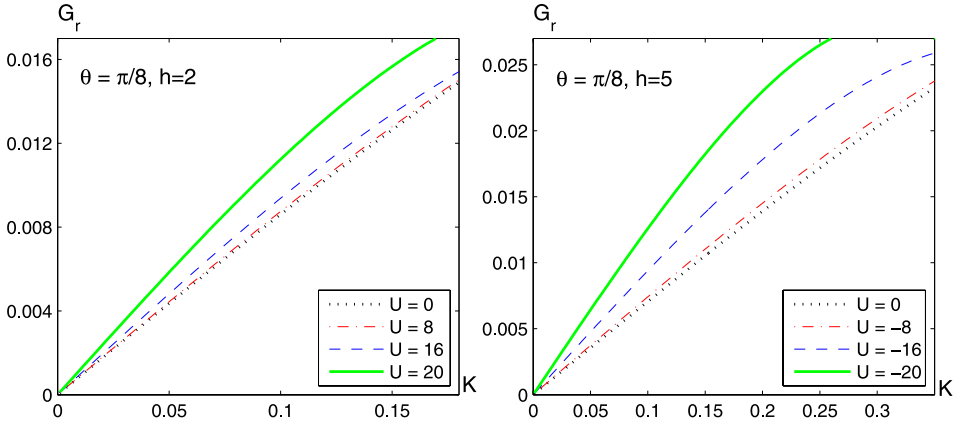

FIGURE 10. G_r vs K, $r = 0.00129$, $A_0 = 0.12$, $B_0 = 0.07$, $\theta = \pi/8$, $h = 2$, $U = 0, 8, 16, 20$ (left), $h = 5$, $U = 0, -8, -16, -20$ (right).

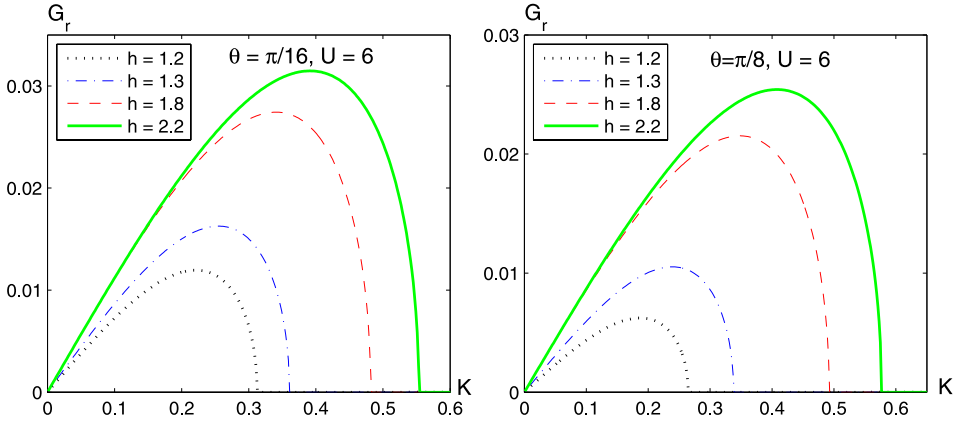

FIGURE 11. G_r vs K, $r = 0.00129$, $A_0 = 0.12$, $B_0 = 0.07$, $U = 6$, $h = 1.2, 1.3, 1.8, 2.2$, $\theta = \pi/16$ (left), $\theta = \pi/8$ (right).

In particular, in Figure 9 the growth rate curve beyond $k = 0.5$ for $h = 2$ and beyond $k = 0.8$ for $h = 5$, cannot be considered to be meaningful.

5. Conclusions

In order to study the effect of uniform wind flow in a situation of crossing sea states over finite-depth water, we have derived nonlinear evolution equations correct up to third order in wave steepness. We have also made stability analysis of a pair of obliquely propagating Stokes wave trains. Note that in the perturbed wave number plane, the region of instability increases with the increase in depth of water medium. The growth rate of instability of one wave train increases with the increase in wave

https://doi.org/10.1017/S1446181118000172 Published online by Cambridge University Press

steepness of the second wave train. We find that the growth rate of instability becomes higher as the two wave trains interact making smaller angles. Figures plotted here show that the growth rate of instability increases with the increase in wind velocity, both for the positive and negative modes of wave propagation. This work may motivate further numerical simulation and experimental investigation in order to expand the horizon of the literature of crossing seas.

To conclude, the limitations of the present model suggest the following works: (i) one may explore a crossing sea states situation above which wind flow is not uniform; (ii) numerical simulation and experimental work may be carried out in order to expand the horizon of the literature of crossing seas.

Appendix A. A_{mn}, A'_{mn}, ζ_{mn}, ζ'_{mn} at the lowest order (in dimensional form)

$$A_{10} = -\frac{i\omega}{k_c \sinh(k_c h)}\left[1 + i\epsilon\left\{\frac{\sigma + k_c h}{\sigma k_c^2}\right\}\left(k\frac{\partial}{\partial x_1} + l\frac{\partial}{\partial y_1}\right) + \frac{i\epsilon}{\omega}\frac{\partial}{\partial t_1}\right]\zeta_{10}, \quad \sigma = \tanh(k_c h)$$

$$A'_{10} = \frac{i(\omega - Uk)}{k_c}\left[1 + \frac{i\epsilon}{k_c^2}\left(k\frac{\partial}{\partial x_1} + l\frac{\partial}{\partial y_1}\right) + \frac{i\epsilon U}{(\omega - Uk)}\frac{\partial}{\partial x_1} + \frac{i\epsilon}{(\omega - Uk)}\frac{\partial}{\partial t_1}\right]\zeta_{10}$$

$$A_{01} = -\frac{i\omega}{k_c \sinh(k_c h)}\left[1 + i\epsilon\left\{\frac{\sigma + k_c h}{\sigma k_c^2}\right\}\left(k\frac{\partial}{\partial x_1} - l\frac{\partial}{\partial y_1}\right) + \frac{i\epsilon}{\omega}\frac{\partial}{\partial t_1}\right]\zeta_{01}$$

$$A'_{01} = \frac{i(\omega - Uk)}{k_c}\left[1 + \frac{i\epsilon}{k_c^2}\left(k\frac{\partial}{\partial x_1} - l\frac{\partial}{\partial y_1}\right) + \frac{i\epsilon U}{(\omega - Uk)}\frac{\partial}{\partial x_1} + \frac{i\epsilon}{(\omega - Uk)}\frac{\partial}{\partial t_1}\right]\zeta_{01}$$

$$\zeta_{20} = F_1\zeta_{10}^2$$

$$A_{20} = i\omega\,\mathrm{cosech}(2k_c h)\left[\sigma^{-1} - \frac{F_1}{k_c}\right]\zeta_{10}^2, \quad A'_{20} = i(\omega - Uk)\left(1 + \frac{F_1}{k_c}\right)\zeta_{10}^2$$

$$\zeta_{02} = F_1\zeta_{01}^2$$

$$A_{02} = i\omega\,\mathrm{cosech}(2k_c h)\left[\sigma^{-1} - \frac{F_1}{k_c}\right]\zeta_{01}^2, \quad A'_{02} = i(\omega - Uk)\left(1 + \frac{F_1}{k_c}\right)\zeta_{01}^2$$

$$\zeta_{11} = F_2\zeta_{10}\zeta_{01}$$

$$A_{11} = \frac{i\omega}{k\sinh(2kh)}\left[\frac{2k^2}{\sigma k_c} - F_2\right]\zeta_{10}\zeta_{01}, \quad A'_{11} = \frac{i(\omega - Uk)}{kk_c}[2k^2 + k_c F_2]\zeta_{10}\zeta_{01}$$

$$\zeta_{1-1} = F_3\zeta_{10}\zeta_{01}^*, \quad A_{1-1} = 0, \quad A'_{1-1} = 0$$

$$F_1 = \frac{2k_c}{f_1}\left[\omega^2 + r(\omega - Uk)^2 - \omega^2\left\{\frac{1 + 2\cosh(2k_c h)}{2\sinh^2(k_c h)}\right\}\right], \quad f_1 = -D(2\omega, 2k, 2l)$$

$$F_2 = \frac{2k}{f_2 k_c^2}[\omega^2\{3k_c^2 - (k^2 - l^2)\sigma^{-2} - 4kk_c\sigma^{-1}\coth(2kh)\}$$
$$+ 2\rho(\omega - Uk)^2(-k^2 - 2l^2 + 2kk_c)], \quad f_2 = -D(2\omega, 2k, 0)$$

$$F_3 = \frac{1}{g(1 - r)}\left[\omega^2 - \omega^2\left(\frac{k^2 - l^2}{\sigma^2 k_c^2}\right) - \frac{2l^2}{k_c^2}r(\omega - Uk)^2\right].$$

https://doi.org/10.1017/S1446181118000172 Published online by Cambridge University Press

Appendix B. Coefficients of the evolution equations

$$\beta_1 = [ks_2 + 2rU(\omega - Uk)]/s_1, \quad \beta_2 = ls_2/s_1$$

$$s_1 = 2\{\omega\sigma^{-1} + r(\omega - Uk)\}, \quad s_2 = -\omega^2 h(1-\sigma^{-2}) + (1-r)\sigma^{-1}$$

$$\beta_3 = -\frac{1}{s_1}\Big[(r+\sigma^{-1})\Big\{k\frac{s_2}{s_1} + 2rU\Big(\frac{\omega - Uk}{s_1}\Big)\Big\}^2 - 2\{-\omega hk(1-\sigma^{-2}) + Ur\}$$
$$\times\Big\{k\frac{s_2}{s_1} + 2rU\Big(\frac{\omega - Uk}{s_1}\Big)\Big\} - \omega^2h^2k^2\sigma^{-1}(1-\sigma^{-2}) - \frac{s_2l^2}{2} + rU^2\Big]$$

$$\beta_4 = -\frac{1}{s_1}\Big[l^2(r+\sigma^{-1})\Big(\frac{s_2}{s_1}\Big)^2 - \omega hl^2(1-\sigma^{-2})\Big\{\frac{h\omega}{\sigma} - 2\Big(\frac{s_2}{s_1}\Big)\Big\} - \frac{s_2k^2}{2}\Big]$$

$$\beta_5 = -\frac{1}{s_1}\Big[2l(r+\sigma^{-1})\Big(\frac{s_2}{s_1}\Big)\Big\{k\frac{s_2}{s_1} + 2rU\Big(\frac{\omega - Uk}{s_1}\Big)\Big\} - 2\omega hkl(1-\sigma^{-2})\Big\{\frac{h\omega}{\sigma} - 2\Big(\frac{s_2}{s_1}\Big)\Big\}$$
$$+ 4rU\omega hl\Big(\frac{\omega - Uk}{s_1}\Big)(1-\sigma^{-2}) - 2rUl\Big(\frac{s_2}{s_1}\Big) + kls_2\Big]$$

$$\lambda_1 = -\frac{1}{s_1}\Big[\{\omega^2(1-\sigma^{-2}) - 2\omega^2(1+\sigma^{-2}) + 2\omega^2 + 2r(\omega - Uk)^2\}F_1$$
$$+ 2\omega^2\sigma^{-1}(\sigma^{-2} - 2) - 2r(\omega - Uk)^2 + \frac{\omega^4(\sigma - \sigma^{-1})^2}{\sigma(1-r)}\Big]$$

$$F_1 = \frac{2}{f_1}\Big[\omega^2 + r(\omega - Uk)^2 - \omega^2\Big\{\frac{1 + 2\cosh(2h)}{2\sinh^2(h)}\Big\}\Big]$$

$$f_1 = -4\omega^2\{\coth(2h) + r\} + 8rU\omega k - 4rU^2k^2 + 2\sigma^{-1}(1-r)$$

$$\lambda_2 = -\frac{1}{s_1}[3\omega^2 - r(\omega - Uk)^2 - (k^2 - l^2)\{\omega^2\sigma^{-2} - r(\omega - Uk)^2\}$$
$$- 4\omega^2\sigma^{-1}k\coth(2kh) + 2r(2k-1)(\omega - Uk)^2]F_2$$
$$- \frac{1}{s_1}[\omega^2 - r(\omega - Uk)^2 - (k^2 - l^2)\{\omega^2\sigma^{-2} - r(\omega - Uk)^2\}]F_3$$
$$+ \frac{2k^2}{s_1}[2\omega^2\sigma^{-1}\{1 - 2k\sigma^{-1}\coth(2kh)\} + 2r(1-2k)(\omega - Uk)^2]$$
$$- \frac{1}{s_1}\Big[4(-2k^2 + l^2)\{\omega^2\sigma^{-1} + r(\omega - Uk)^2\} + \frac{\omega^4(\sigma - \sigma^{-1})^2}{\sigma(1-r)}\Big]$$

$$F_2 = \frac{2k}{f_2}[\omega^2\{3 - (k^2 - l^2)\sigma^{-2} - 4k\sigma^{-1}\coth(2kh)\} + 2r(\omega - Uk)^2(-k^2 - 2l^2 + 2k)]$$

$$f_2 = -4\omega^2\{\coth(2kh) + r\} + 8rU\omega k - 4rU^2k^2 + 2k\sigma^{-1}(1-r)$$

$$F_3 = \frac{\sigma}{(1-r)}[\omega^2 - \omega^2\sigma^{-2}(k^2 - l^2) - 2l^2r(\omega - Uk)^2]$$

$$\lambda_3 = \frac{1}{\sigma s_1(1-r)}, \quad \mu_1 = \sigma^2\beta_1^2 - (1-r)\sigma h, \quad \mu_2 = -(1-r)\sigma h.$$

https://doi.org/10.1017/S1446181118000172 Published online by Cambridge University Press

References

[1] W. Bascom, *Waves and beaches: The dynamics of the ocean surface* (Anchor Books, Doubleday, 1980).

[2] L. F. Bliven, N. E. Huang and S. R. Long, "Experimental study of the influence of wind on Benjamin–Feir sideband instability", *J. Fluid Mech.* **162** (1986) 237–260; doi:10.1017/S0022112086002033.

[3] M. Brunetti and J. Kasparian, "Modulational instability in wind-forced wave", *Phys. Lett.* A **378** (2014) 3626–3630; doi:10.1016/j.physleta.2014.10.017.

[4] A. Chabchoub, "Tracking breather dynamics in irregular sea state conditions", *Phys. Rev. Lett.* **117** (2016) 144103; doi:10.1103/PhysRevLett.117.144103.

[5] A. Chabchoub, N. Hoffmann, H. Branger, C. Kharif and N. Akhmediev, "Experiments on wind-perturbed rogue wave hydrodynamics using the Peregrine breather model", *Phys. Fluids* **25** (2013) 101704; doi:10.1063/1.4824706.

[6] A. Davey and K. Stewartson, "On three dimensional packets of surface waves", *Proc. R. Soc. Lond.* **A338** (1974) 101–110; doi:10.1098/rspa.1974.0076.

[7] S. Debsarma, S. Kundu and K. P. Das, "Modulational instability of two crossing waves in the presence of wind flow", *Ocean Model.* **94** (2015) 27–32; doi:10.1016/j.ocemod2015.07.017.

[8] S. Debsarma, S. Senapati and K. P. Das, "Wind-forced modulations in crossing sea states over infinite depth water", *Phys. Fluids* **26** (2014) 096606; doi:10.1063/1.4896031.

[9] A. K. Dhar and K. P. Das, "A fourth-order evolution equation for deep water surface gravity waves in the presence of wind blowing over water", *Phys. Fluids* **A2** (1990) 778–783; doi:10.1063/1.857731.

[10] A. K. Dhar and K. P. Das, "Fourth order nonlinear equation for two stokes wave trains in deep water", *Phys. Fluids* **A 3** (1991) 3021–3026; doi:10.1063/1.858209.

[11] A. I. Dyachenko and V. E. Zakharov, "Modulation instability of Stokes wave → Freak wave", *JETP Lett.* **81** (2005) 255–259; doi:10.1134/1.1931010.

[12] K. Dysthe, H. E. Krogstad and P. Muller, "Oceanic rogue waves", *Annu. Rev. Fluid Mech.* **40** (2008) 287–310; doi:40.111406.10220.

[13] O. Gramsted, H. Zeng, K. Trulsen and G. K. Pedersen, "Freak waves in weakly nonlinear unidirectional wave trains over a slopping bottom in shallow water", *Phys. Fluids* **25** (2013) 122103; doi:10.1063/1.4847035.

[14] P. Janssen, *The interaction of ocean waves and wind* (Cambridge University Press, Cambridge, 2004); ISBN-13: 978-0521121040, ISBN-10: 0521121043.

[15] C. Kharif, J. P. F. J. T. Giovanangeli, L. Grare and L. Pelinovsky, "Influence of wind on extreme wave events: experimental and numerical approaches", *J. Fluid Mech.* **594** (2008) 209–247; doi:10.1017/S0022112007009019.

[16] C. Kharif and E. Pelinovsky, "Physical mechanism of the rogue wave phenomenon", *Eur. J. Mech. B Fluids* **22** (2003) 603–634; doi:10.1016/j.euromechflu.2003.09.002.

[17] C. Kharif, E. Pelonovsky and A. Slunyaev, *Rogue waves in the ocean* (Springer, New York, 2009); ISBN: 978-3-540-88418-7.

[18] S. Kundu, S. Debsarma and K. P. Das, "Modulational instability in crossing sea states over finite depth water", *Phys. Fluids* **25** (2013) 066605; doi:10.1063/1.4811695.

[19] S. Leblanc, "Amplification of nonlinear surface waves by wind", *Phys. Fluids* **19** (2007) 101705; doi:10.1063/1.2786002.

[20] S. Leblanc, "Wind-forced modulations of finite-depth gravity waves", *Phys. Fluids* **20** (2008) 116603; doi:10.1063/1.3026551.

[21] J. W. Miles, "On the generation of surface waves by shear flows", *J. Fluid Mech.* **3** (1957) 185–204; doi:10.1017/s0022112057000567.

[22] J. W. Miles, "On the generation of surface waves by turbulent shear flows", *J. Fluid Mech.* **7** (1960) 469–478; doi:10.1017/s0022112060000220.

[23] M. Onorato, A. R. Osborne and M. Serio, "Modulational instability in crossing sea states: A possible mechanism for the formation of freak waves", *Phys. Rev. Lett.* **96** (2006) 014503; doi:10.1103/PhysRevLett.96.014.
[24] M. Onorato and D. Proment, "Triggering rogue waves in opposing currents", *Phys. Rev. Lett.* **107** (2011) 184502; doi:10.1103/PhysRevLett107.114502.
[25] M. Onorato, S. Residori, U. Bertolozzo, A. Montina and F. T. Arecchi, "Rogue waves and their generating mechanisms in different physical contexts", *Phys. Rep.* **528** (2013) 47–89; doi:10.1016/j.physrep.2013.03.
[26] W. L. Peirson and A. W. Garcia, "On the wind-induced growth of slow water waves of finite steepness", *J. Fluid Mech.* **608** (2008) 243–278; doi:10.1017/S002211200800205X.
[27] V. P. Ruban, "On the nonlinear Schrödinger equation for waves on a nonuniform current", *JETP Lett.* **95** (2012) 486–491; doi:10.1134/S002136401209010X.
[28] S. Senapati, S. Kundu, S. Debsarma and K. P. Das, "Nonlinear evolution equations in crossing seas in the presence of uniform wind flow", *Eur. J. Mech. B Fluids* **60** (2016) 110–118; doi:10.1016/j.euromechflu2016.06.014.
[29] P. K. Shukla, I. Kourakis, B. Eliasson, M. Marklund and L. Stenflo, "Instability and evolution of nonlinear interacting water waves", *Phys. Rev. Lett.* **97** (2006) 094501; doi:10.1103/PhysRevLett.97.094.
[30] A. Toffoli, D. Proment, H. Salman, J. Monbaliu, F. Frascoli, M. Dafilis, E. Stramignoni, R. Forza, M. Manfrin and M. Onorato, "Wind generated rogue waves in an annular wave flume", *Phys. Rev. Lett.* **118** (2017) 144503; doi:10.1103/PhysRevLett.118.144503.
[31] A. Toffoli, T. Waseda, H. Houtani, T. Kinoshita, K. Collins and D. Proment, "Excitation of rogue waves in a variable medium: An experimental study on the interaction of water waves and currents", *Phys. Rev. Lett.* **E87** (2013) 051201(R); doi:10.1103/PhysRevE.87.051201.
[32] T. Waseda and M. P. Tulin, "Experimental Study of the stability of deep-water wave trains including wind effects", *J. Fluid Mech.* **401** (1999) 55–84; doi:10.1017/S00221120990-06527.